



Hybrid optimization techniques based automatic artificial respiration system for corona patient

S. Sakthiya Ram ^a, C. Kumar ^b, A. Ramesh Kumar ^c and T. Rajesh ^a

^aBannari Amman Institute of Technology, Sathyamangalam, Tamil Nadu, India; ^bM. Kumarasamy College of Engineering, Karur, Tamil Nadu, India; ^cSt. Joseph's Institute of Technology, Chennai, Tamil Nadu, India

ABSTRACT

Artificial ventilation is widely used for various respiratory problems of human beings. The oxygen level of the corona patients has to be maintained for smooth breathing which is very difficult. For achieving this state, the air pressure should be controlled in the respiration system that has a piston mechanism driven by a motor. An Automatic respiration system model is designed and controller parameters are tuned using hybrid Optimization techniques. Hybrid Controllers like genetic algorithm based Fractional Order Proportional Integral Derivative controller (FOPID), Fmincon-Pattern search Algorithm based Proportional Integral Derivative (PID) controller, and Hybrid Model predictive control (MPC) – Proportional Integral Derivative (PID) controllers were designed and verified. Integral Square Error is considered as the objective function of the optimization technique to find the controller parameters. The output responses of all three hybrid controllers are compared based on the error indices, time domain specifications, set-point tracking and Convergence speed graph. The genetic algorithm-based FOPID controller gives better results when compared with the Fmincon-Pattern search Algorithm based Proportional Integral Derivative (PID) controller and Hybrid Model predictive control (MPC) – Proportional Integral Derivative (PID) for the proposed artificial ventilation system.

ARTICLE HISTORY

Received 22 June 2021
Accepted 14 January 2022

KEYWORDS

Artificial respiration; genetic algorithm; Fmincon; pattern search; hybrid MPC-PID; FOPID

1. Introduction

COVID-19 is one of the major respiratory diseases that started to spread in November 2019. The Corona Virus reaches the lungs of human, the respiratory tract and starts to multiply. This issue may block the lungs and create breathing problems ranging from mild to severe based on the health conditions of the patient. Coronavirus may severely affect elderly people who already have other health problems, such as heart-related disease, asthma, and diabetes. The coronavirus family contains SARS-CoV-2, the virus that activates COVID-19 [1]. When the virus enters into the good and healthy cells, it multiplies and attacks the neighbouring cells. The illness spreads across the respiratory tract, where the immune system fights back. They swell and become inflamed in the lungs and airways. About 80% of people who have COVID-19 have symptoms that are mild to moderate. Patients affected by coronavirus may have a loss of smell, dry cough, loss of taste, cold and increase in temperature. With a chest X-ray or CT scan, doctors can show symptoms of lung inflammation called Ground Glass Opacity. The ground-glass opacity is a hazy grey region that can be seen in CT scans [2]. The increasing density inside the lungs is indicated by these grey spots. The patients will face severe difficulties in breathing when they do not take proper medicines in

the starting stage. When the oxygen level reduces below 90%, the patients can breathe only with the help of a mechanical ventilator or artificial ventilator [3,4].

An artificial respiration system will replace the respiratory muscles that provide the energy required during the inspiration process to ensure the flow of gas into the alveoli ducts [5]. With the help of the artificial ventilation system, the patient can breathe easily and this makes it easy for doctors to reduce the cold that has blocked the lungs. The oxygen level or oxygen saturation level of the patient will be monitored using Pulse oximeters often to know the amount of oxygen level to be supplied for the patient. The doctors found it difficult when a large number of patients were admitted due to the fast spread of Coronavirus. The Auto respiration system helps the doctors by automatically tuning the desired output based on the amount of oxygen required by the patients. An air section with a piston system driven by the motor is the main component of an artificial respiration system. The piston direction is changed by the control mechanism. The finest value of the constraints configuration on the artificial respiration device is the difficult challenge since a patient's ventilator parameters depend on several variables. For its good quality, modest control appliance, and good performance, the optimization algorithm-based artificial

CONTACT S. Sakthiya Ram sakthiyaram@bitsathy.ac.in

This article has been corrected with minor changes. These changes do not impact the academic content of the article.

ventilation system is therefore becoming more popular. Patients decide their respiratory rate during aided respiration, but the ventilator decides the tidal volume. In regulated breathing, the ventilator determines both the rate of respiration and tidal length [6]. Each ventilation model has different configuration ranges. More modern and developed machines offer more options for operators in respiratory settings.

Swarm-based optimization techniques were used for designing PID controllers for artificial respiration systems. The Constricted Class Topper Optimization algorithm gives better results when compared to Class Topper Optimization and Particle Swarm Optimization techniques [7]. The self-adaptive particle swarm optimization is designed for the selection of a wide range of features. The SaPSO gives better results in terms of classification accuracy than Evolutionary and Non Evolutionary computation counterparts [8]. A mechanical ventilator is designed and examined to implement the control methods that help researchers by outlining new trends. Classical and Intelligent control ventilators have been designed using volume, time, pressure, and flow [9]. The Fuzzy Logic-based controller is considered for controlling the pressure in a mechanical ventilator system. It is concluded that the Fuzzy algorithm-based controller has the ability to regulate the level of pressure support ventilation from continuous measurements of a patient's vital signs [10]. The dual closed-loop control system is designed for the mechanical ventilation system. To automatically change the oxygen concentration in the patient's intake air, the controller uses the response from the patient's arterial oxygen saturation and combines a rapid stepwise monitoring protocol with a PID control algorithm [11]. For patients on mechanical ventilation, a method for controlling the fraction of inspired oxygen (F(IO₂)) and positive end-expiratory pressure (PEEP) is designed. F(IO₂) is regulated in this method by two interacting mechanisms: a fine control mechanism and a rapid stepwise protocol that is used when the patient's oxygen saturation level (S(pO₂)) drops suddenly [12].

A method based on hybrids of machine learning and nature-inspired algorithms to improve current time-series prediction (forecasting) technologies is proposed [13]. The suggested prediction model combines machine learning, adaptive neuro-fuzzy inference, adaptive neuro-fuzzy inference system, and enhanced beetle antennae search swarm intelligence metaheuristics. The increased beetle antennae search is used to select the adaptive neuro-fuzzy inference system's parameters and to improve the prediction model's overall performance. The suggested hybrid method outperformed other advanced algorithms tested on the same datasets, proving to be a helpful tool for time-series prediction, according to simulation findings and comparison analysis.

Soft-computing-based optimization technology is currently being used to solve various forms of research problems [14]. In the field of biomedical engineering, optimization-based technology can be used to solve multiple problems. The contribution of this paper is to design the controller for the Airway Pressure in the Auto Respiration System. To tune the controller values for various types of control problems, Hybrid Model Predictive Controller, genetic algorithm-based Fractional Order PID, Fmincon-pattern search based PID controllers have been considered. The Airway Pressure of the ventilation system has to be tuned. Here the closed-loop ventilation control is implemented. The model is designed based on the first principle method and the optimization techniques are implemented to control the airway pressure. The optimization techniques are compared based on the time domain specification, error indices, set-point tracking, and convergence speed graph to find the best controller to be used to tune the Airway Pressure of the Respiration system [15,16]. Integral Square Error (ISE) is used as the objective function for the optimization techniques used. ISE is used as an objective function to limit the PID parameter gain values for the fast processes. It also reduces the large errors [17]. In the future, the dataset of the patients may be collected and the model is trained using machine learning techniques and an optimized convolutional neural network may be used to tune the controller [18].

2. Process description

The Artificial respiration system consists of sensors, displaying equipment, and a control mechanism for the continuous monitoring of corona patients. The basic block diagram of the model is represented in Figure 1. The airway pressure that is needed to be controlled is given as input and the desired or controlled pressure will be the output. The electric motor present here will be used to operate the piston movement. Figure 2 represents the block diagram of the artificial respiration system. Here, the main objective is to control the Airway Pressure inside the air compartment of the artificial respiration system. Initially, the air reaches the body from the nose or mouth and flows down to the throat through the larynx and trachea. Then, by the main stem called bronchi, they are accessible in both left and right lungs, it joins the lungs. These primary stems in the lungs split into smaller stems and split into further smaller tubes called the bronchioles [19]. Small air sacs called alveoli to end with these bronchioles. Each lung has several million alveoli, and these areas are responsible for the exchange of gases. Each alveolus interacts closely with a capillary network containing pulmonary artery deoxygenated blood.

The respiratory sensor that is connected to the controller [20] detects the respiratory output from the

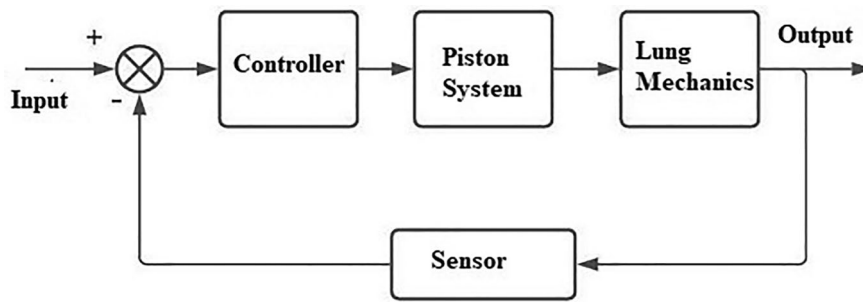


Figure 1. The basic block diagram of the model.

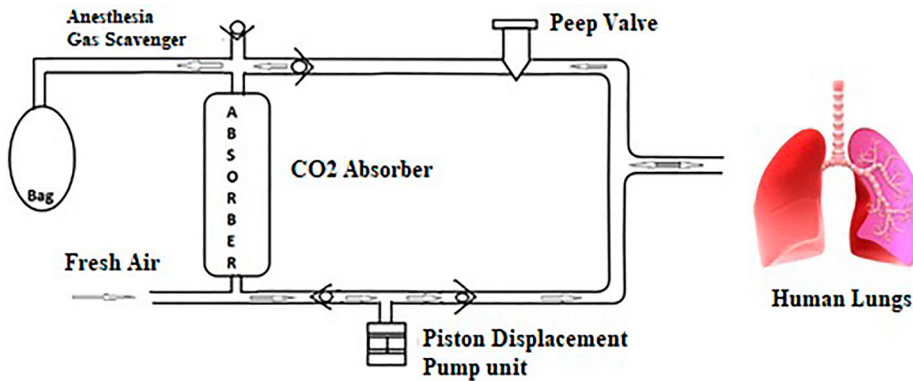


Figure 2. The block diagram of the artificial respiration system.

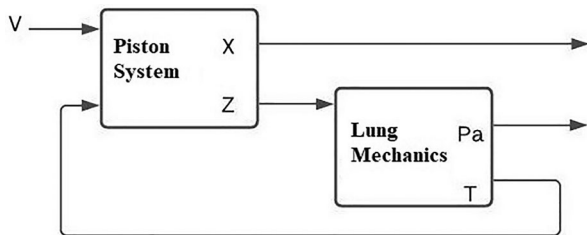


Figure 3. The system dynamics of breathing mechanics.

human body. The controller delivers the necessary amount of oxygen to the lungs based on the level of the oxygen required [21]. The airway pressure control is concentrated here. The Airway pressure (P_a) is determined by Pneumatic resistance and Lung storage capacity. When considering the gain of the current control

[22] loop of the piston drive mechanism, the time constant of the system is noted as a first-order differential system [23].

The Piston system and Lung Mechanic are two major sub-components of the artificial respiration system [24]. The system dynamics of breathing mechanics are represented in Figure 3 where Z is the piston speed, V is the input voltage to the system, X is the output of the piston drive system, P_a is the airway pressure and T is the load torque. The Auto respiration system model is designed based on the control loop gain, control loop time, field flux, the moment of inertia, piston area, coefficient of friction, the transmission of the piston drive system and Pneumatic resistance, Lung storage capacity of the lung mechanics [7]. The Piston drive system block diagram is shown in Figure 4.

Table 1 represents the symbol used in the respiratory system's open loop model.

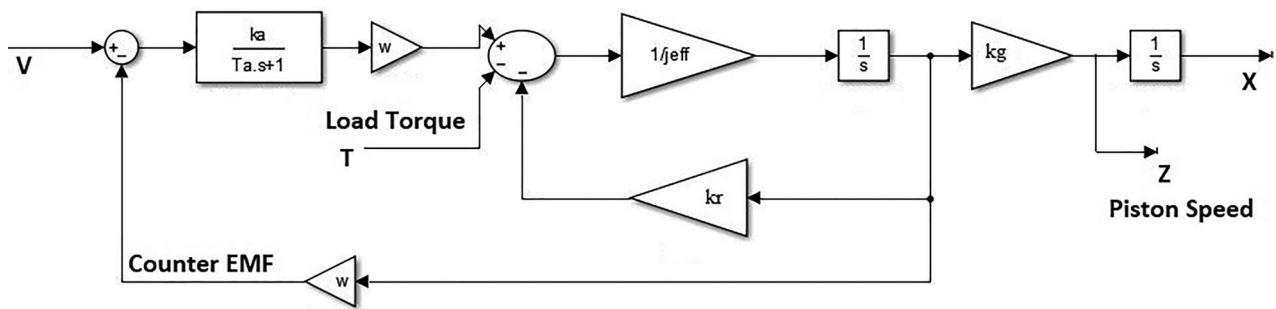


Figure 4. Piston system block diagram.

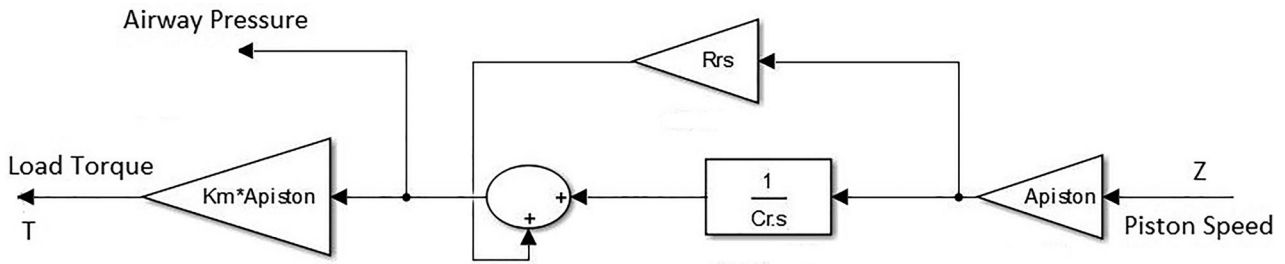


Figure 5. Lung mechanics block diagram.

Table 1. The symbol and values used in the respiratory system's open loop transfer function model.

Symbol	Description	Values
k_a	Current control loop Gain	0.368 A/V
T_a	Current control loop Time	9e-5
w	Field flux	2.79 Ncm/A
J_{eff}	Moment of inertia	0.0032 N cm s ²
A_{piston}	Area of the Piston	1.62 dm ²
k_r	Coefficient of friction	0.005 N cm/rad
k_g	Transmission	0.4 mm/rad
R_r	Pneumatic resistance	2 mbar s/l
C_r	Lung Storage capacity	70 ml/mbar
K_m	Transfer ratio	0.0391 cm

The first-order differential equation can be used to express the motor's time constant. In a piston-motor driving system, friction is considered linear. The applied motor voltage is the input variable for the piston-motor driving system. The load torque feedback from the lung system is also fed into the piston-motor drive system. The torque balance equation is represented in Equation (1).

$$j_{eff} \cdot \omega = T + \frac{k_a}{1 + T_a s} V - w^2 \frac{k_a}{1 + T_a s} \omega - k_r \cdot \omega \quad (1)$$

where V is the input voltage, T is load Torque, k_a is current control loop gain, T_a is current control time constant, k_r is the coefficient of friction, w is field flux, j_{eff} is the moment of inertia. The Lung Mechanics block diagram is shown in Figure 5.

The mathematical derivation of the lung mechanics shown in Figure 5 in Laplace domain is shown in Equation (2)

$$T = K_m \cdot A_{piston}^2 \cdot \left(R_r + \frac{1}{C_r \cdot S} \right) \cdot Z \quad (2)$$

where A_{piston} is the area of the piston, K_m is transfer ratio, C_r is lung storage capacity and R_r is Pneumatic resistance of lungs and Z is the piston speed. The respiratory system's open loop model is shown in Figure 6.

Table 2 represents the lung parameters in comparison with the age [24]. The Storage capacity of the lungs increases with age and Pneumatic resistance decreases with age. Here, the Automatic Respiration System is designed for adults.

Table 2. The Lung parameters for different age groups.

Age groups	C_r (ml/mbar)	R_r (mbar s/l)
New Born	3-5	30-50
Infant	10-15	20-30
Kids	20-40	10
Adults	70-100	2-4

A patient feedback control loop is considered when designing an artificial ventilator controller. The interaction of the patient with the system can be considered a disturbance. The desired pressure is sent to the controller as the reference signal. A controller is used to illustrate the closed-loop model in a block diagram shown in Figure 7.

The values of the respiration system parameters represented in Table 1 are loaded to execute the model. A mathematical model is designed using the first principle method [25,26]. This idea is very helpful as the Airway Pressure that is to be controlled will vary according to the patient of different ages and also vary if they are affected by corona [27]. So the C_r and R_r values can be varied whenever necessary to control the Airway Pressure.

3. Controller design

The Airway Pressure in the Auto Respiration System is controlled using controllers like Hybrid Fmincon-pattern search algorithm based PID controller, genetic algorithm-based FOPID controller, and Hybrid MPC-PID controllers using MATLAB.

3.1. Hybrid Fmincon-pattern search based PID controller

The block diagram of the Hybrid optimization-based PID controller is shown in Figure 8. Here, the airway pressure is given as the input and output will be the desired or controlled pressure value. The optimization techniques are used to tune the PID parameters of the Auto Respiration System. Using the interior-point algorithm, the Fmincon (Find the minimum of constrained) algorithm is used to find the minimum of a constrained nonlinear multivariable equation. The algorithm selected here is 'interior-point' that handles

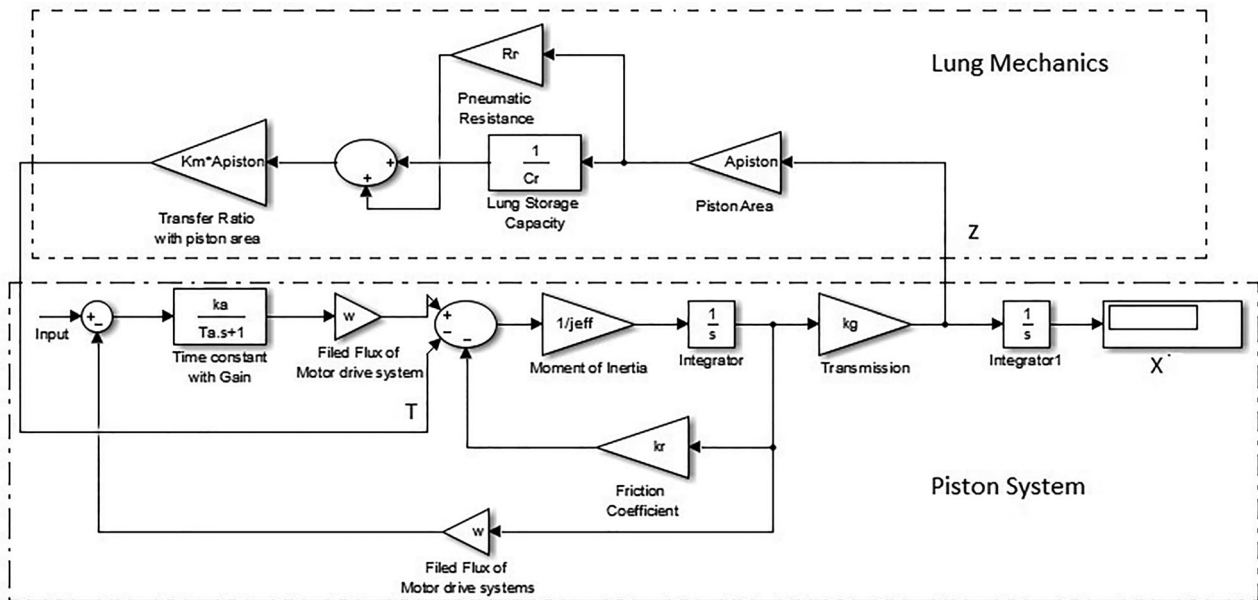


Figure 6. The respiratory system's open loop model.

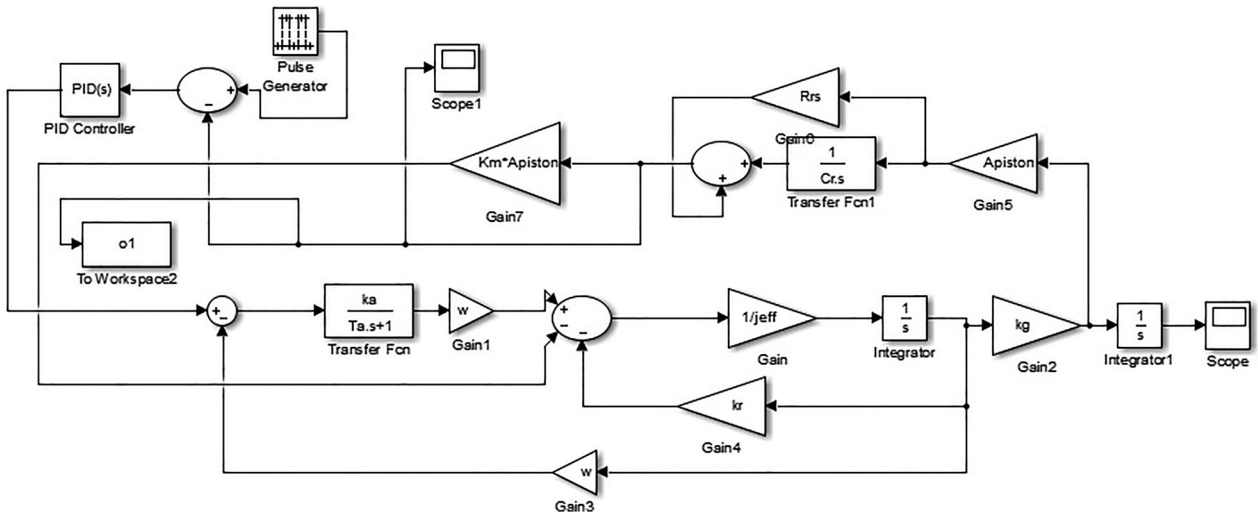


Figure 7. The respiratory system's closed loop transfer function model.

sparse problems, large, as well as small intense problems. The Fmincon algorithm compensates the bounds at all iterations and also can improve from NaN or Inf results [28]. This algorithm can use some special techniques for large-scale issues. The Fmincon Algorithm Flowchart is shown in Figure 9.

In the Fmincon algorithm process, the input value is given which includes the Active powers, Constraints and Starting point x_0 . Based on the constraints given, an evaluation process takes place. J is considered as the Fmincon function. Then Iteration (iter) will be increased and new values of K_p , K_d , K_i values will be selected within the range of the constraints. The present Fmincon function $J(x_i)$ is compared with the previous value $J(x_{i-1})$. The iteration will be repeated until the best optimum value of K_p , K_d , K_i value is reached or if the iteration reaches the maximum value.

The objective function is considered as Integral Square Error (ISE). Equation (3) represents the ISE,

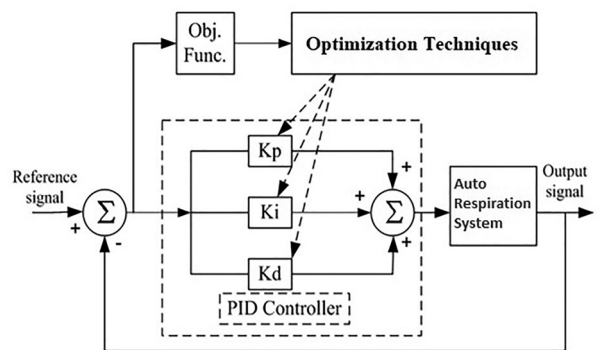


Figure 8. The block diagram of the Hybrid optimization based PID controller.

where, $e(t)$ is the error that is the difference between the actual and desired pressure value.

$$ISE = \int_0^T e(t)^2 dt \tag{3}$$

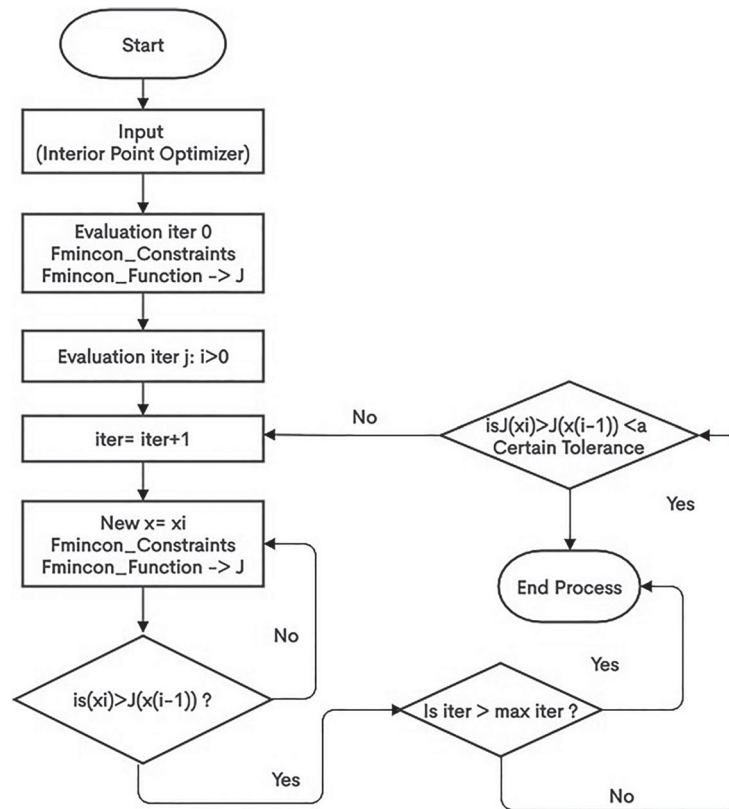


Figure 9. Fmincon algorithm flowchart.

The initial value is considered as $X = (X1, X2, X3)$. MATLAB Equations (4)–(6) returns the values of the PID parameter based on the objective function ISE.

$$\begin{aligned}
 & [Kp, fv1, ef1, op1, L, G, H] \\
 & = f(\text{ISE}, X1, A1, b1, Aeq1, beq1, lb1, ub1, N1, O1)
 \end{aligned} \quad (4)$$

$$\begin{aligned}
 & [Ki, fv2, ef2, op2, L, G, H] \\
 & = f(\text{ISE}, X2, A2, b2, Aeq2, beq2, lb2, ub2, N2, O2)
 \end{aligned} \quad (5)$$

$$\begin{aligned}
 & [Kd, fv3, ef3, op3, L, G, H] \\
 & = f(\text{ISE}, X3, A3, b3, Aeq3, beq3, lb3, ub3, N3, O3)
 \end{aligned} \quad (6)$$

In Equations (4)–(6), the algorithm starts with the initial value and finds the minimum value of the function based on the objective function ISE. In MATLAB, Equations (4)–(6) fmincon is abbreviated as f , the final value is abbreviated as fv , exit flag is abbreviated as ef , the output is abbreviated as op , L represents the structure of fields comprising the Lagrange multipliers, G represents the Gradient of the objective function of PID parameter. A , b are the linear inequality constraints matrix and vector, respectively. Aeq and beq are the linear equality constraints matrix and vector, respectively. lb represents the lower bound and ub represents the upper bound for the PID parameters. The $fval$ is nothing but the value of the objective function that

is returned as a real number. H represents the objective function's Hessian of the PID parameter and O represents the option that returns a collection of the optimization problem.

Fmincon also returns a value [8] exit flag that defines the exit state of the algorithm, as well as a structured output that contains details about the optimization process.

The Hessian of the Lagrangian is represented in Equation (7).

$$H = \nabla^2 L = \nabla^2 \text{ISE} + \sum_i \lambda_i \nabla^2 C_i + \sum_j \lambda_j \nabla^2 C_{eqj} \quad (7)$$

where C represents the nonlinear inequality constraint vector and C_{eq} represents the nonlinear equality constraint vector. In Hessian, BFGS (Broyden–Fletcher–Goldfarb–Shanno) algorithm is selected as it is an interactive method that solves the unconstrained nonlinear optimization problems. In the Algorithm setting, set Typical X values that indicate the distinctive magnitude of the variables [8,29]. In the projected conjugate iteration, the maximum iterations indicate the maximum number of projected conjugate gradient iterations. The relative tolerance indicates the relative termination tolerance on the projected conjugate gradient iteration. The absolute tolerance indicates the absolute termination tolerance on the projected conjugate gradient iteration. The stopping criteria indicate the reason for the termination of the algorithm. Max

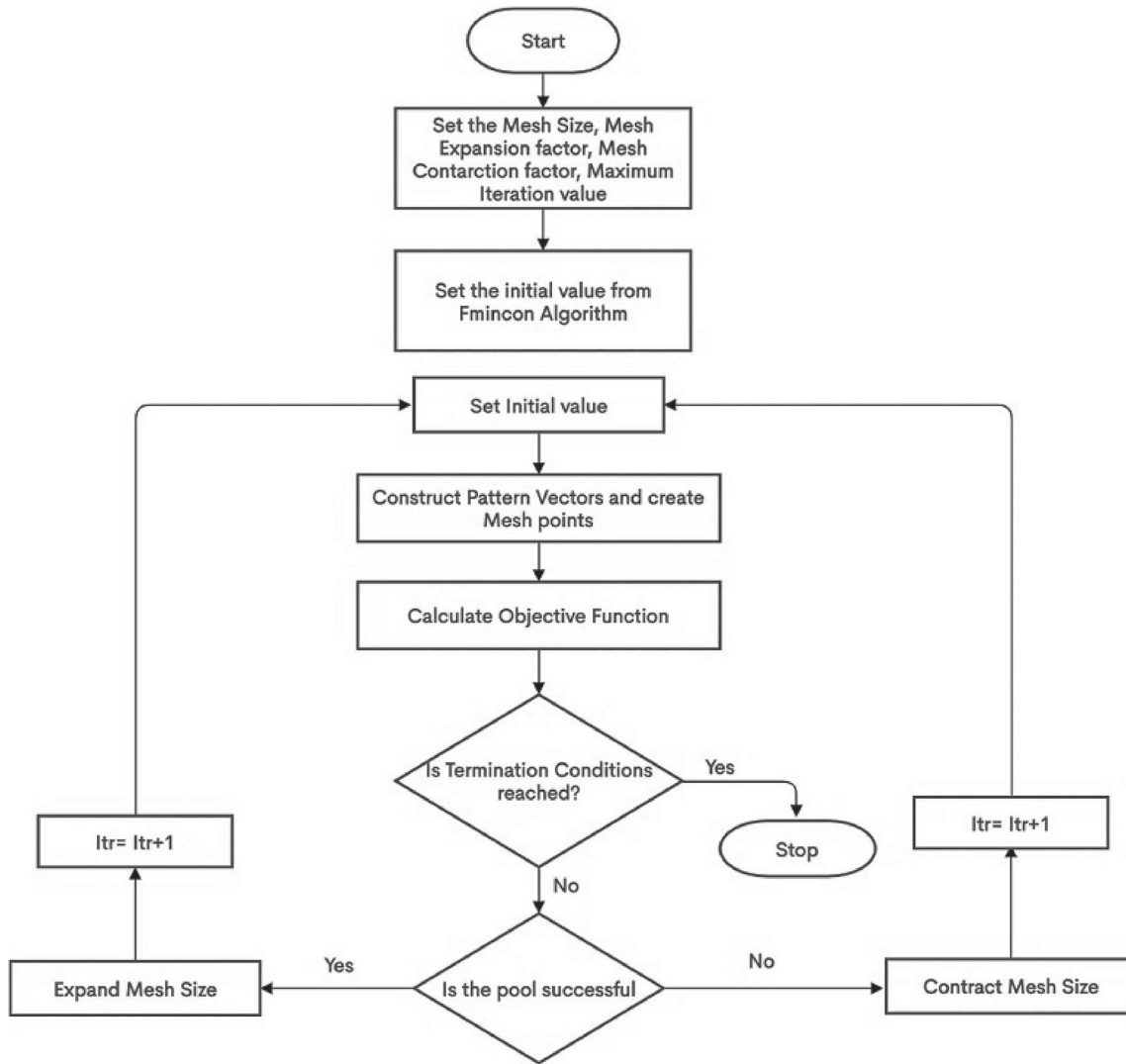


Figure 10. Fmincon-pattern search algorithm flowchart.

iterations indicate the maximum number of iterations that the algorithm will perform. The highest number of evaluations of the constraints and objective function has to be mentioned in Max function evaluations. The algorithm runs for many numbers of iterations until it gets the best fit values. If there is any issue identified, the algorithm terminates and the reason for termination will be displayed.

The best fit value obtained in the Fmincon algorithm will be given as the input for the pattern search algorithm. The pattern search (PS) optimization technique is a derivative-free evolutionary algorithm that can be used to solve a wide range of optimization problems that are outside the limits of traditional optimization techniques [30]. It has a straightforward definition, is simple to enforce, and is computationally efficient [31]. The Hybrid Fmincon-pattern search algorithm flowchart is shown in Figure 10. The Objective function considered here is Integral Square Error (ISE).

The initial value as obtained from Fmincon algorithm is, $X = (X1, X2, X3)$

$$[Kp, fv1, ef1, op1]$$

$$= ps(ISE, X1, A1, b1, Aeq1, beq1, lb1, ub1, N1, O1) \quad (8)$$

$$[Ki, fv2, ef2, op2]$$

$$= ps(ISE, X2, A2, b2, Aeq2, beq2, lb2, ub2, N2, O2) \quad (9)$$

$$[Kd, fv3, ef3, op3]$$

$$= ps(ISE, X3, A3, b3, Aeq3, beq3, lb3, ub3, N3, O3) \quad (10)$$

Here, the algorithm starts with the initial value and finds the minimum value of the function based on the objective function ISE. In the equation, pattern search is abbreviated as *ps*, the final value is abbreviated as *fv*, exit flag is abbreviated as *ef*, the output is abbreviated as *op*. *A*, *b* are the linear inequality constraints matrix and vector, respectively. *Aeq* and *beq* are the linear equality constraints matrix and vector, respectively. *lb* represents the lower bound and *ub* represents the upper bound for the PID parameters.

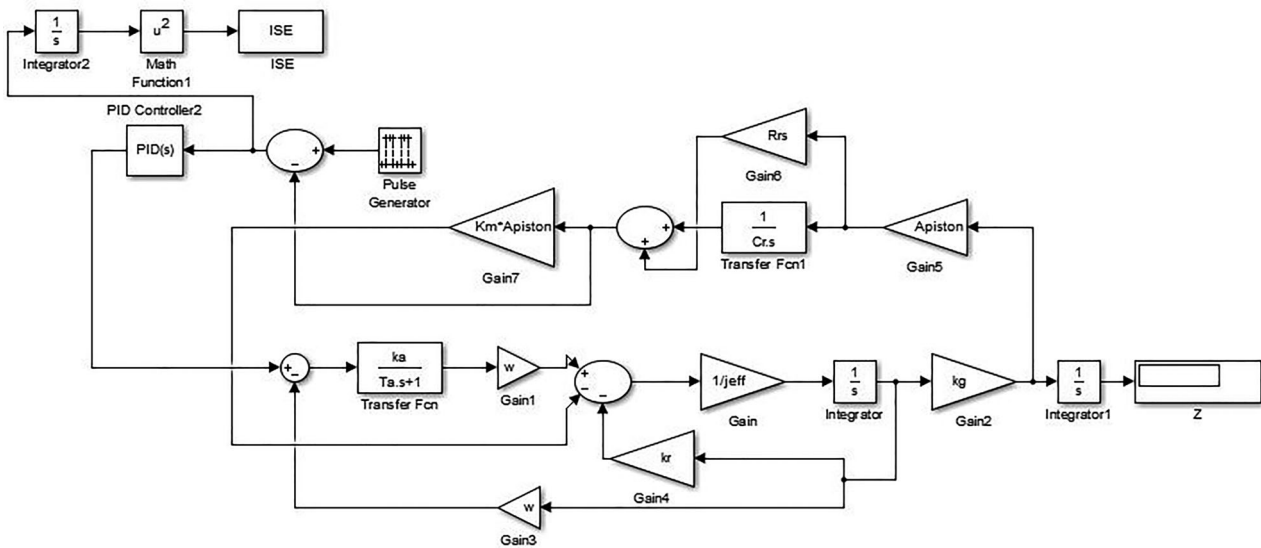


Figure 11. The simulink model of Hybrid Fmincon-Pattern Search based PID Controller.

The fitness function is nothing but the objective function that needs to be reduced has to be specified here. The lower and upper bounds on the variables are to be mentioned in the constraints. The control on how the pattern search will poll the mesh points will be done by Poll options. This option depends on the class of algorithms utilized. Poll Method will indicate the method that the poll algorithm utilized to form the mesh. The Complete poll indicates if all the points are polled in all the iterations in the current mesh. The polling order indicates the order that searches the points in the recent mesh using GSS or GPS methods. Consecutive is selected in the polling order that determines deterministic order. The term search option refers to the algorithm's ability to run searches at any iteration before polling. When the search yields a point that increases the objective property, the algorithm uses the point in subsequent iterations rather than polling. The mesh used for the pattern quest will be controlled by Mesh Options. The initial mesh's size is defined as the length of the vector between the initial point and the mesh point. The initial size must always be a positive scalar. After a good iteration, the mesh size would not rise until the full size has been achieved. The Accelerator indicates if 0.5 is multiplied to the Mesh contraction factor after all the unsuccessful iteration of the smaller mesh size. An Accelerator is applied in the GPS and GSS algorithms. The scale parameter is set to true if the algorithm scales the mesh points by multiplying the pattern vectors by constants relative to the logarithms of the current point's coordinates. The Scale is not utilized when there is an equality constraint. The expansion factor determines how much the mesh size can be expanded after a favourable vote. The Expansion factor should be a positive scalar, and it should only be used for a GPS or GSS poll or search function. The existence of cache in the algorithm is indicated by the Cache choice. The algorithm cannot test the objective function

at any mesh points under the Tolerance if the Cache is turned on. The stopping criteria indicate the reason for the termination of the pattern search algorithm. The Mesh tolerance indicates the minimum tolerance of the size of the mesh. The maximum number of iterations that the algorithm will perform has to be specified in Max Iteration. The highest number of evaluations of the constraints and objective function has to be mentioned in Max function evaluations. The maximum time that the algorithm has to run before terminating should be specified in the Time limit. The algorithm runs for many iterations until it gets the best fit values [32]. If there is any issue identified, the algorithm terminates and the reason for termination will be displayed. The best fit value can be used to tune the Kp , Ki , Kd value of the PID controller [33]. The MATLAB Simulink model of Hybrid Fmincon-Pattern Search based PID Controller is shown in Figure 11. The simulation time is 10 s. PID parameters of Hybrid Fmincon-pattern search based PID controller is tabulated in Table 3.

The Controller response vs Process variable of hybrid Fmincon-PS based PID controller is shown in Figure 12.

3.2. Genetic algorithm based FOPID controller

The genetic algorithm is an optimization technique used to solve constrained and unconstrained issues [34]. It is working based on the natural identification process that is similar to that of the biological process [35]. The well-known and widely used evolutionary algorithms are based on the Darwinian mechanism of evolution, natural selection, and regular genetics [36]. The controller parameters for fractional-order PID controllers, such as proportional gain (Kp), integral time (Ki), derivative time (Kd), fractional order integral term coefficient (λ) and fractional order derivative term coefficient (μ), are calculated using genetic algorithm

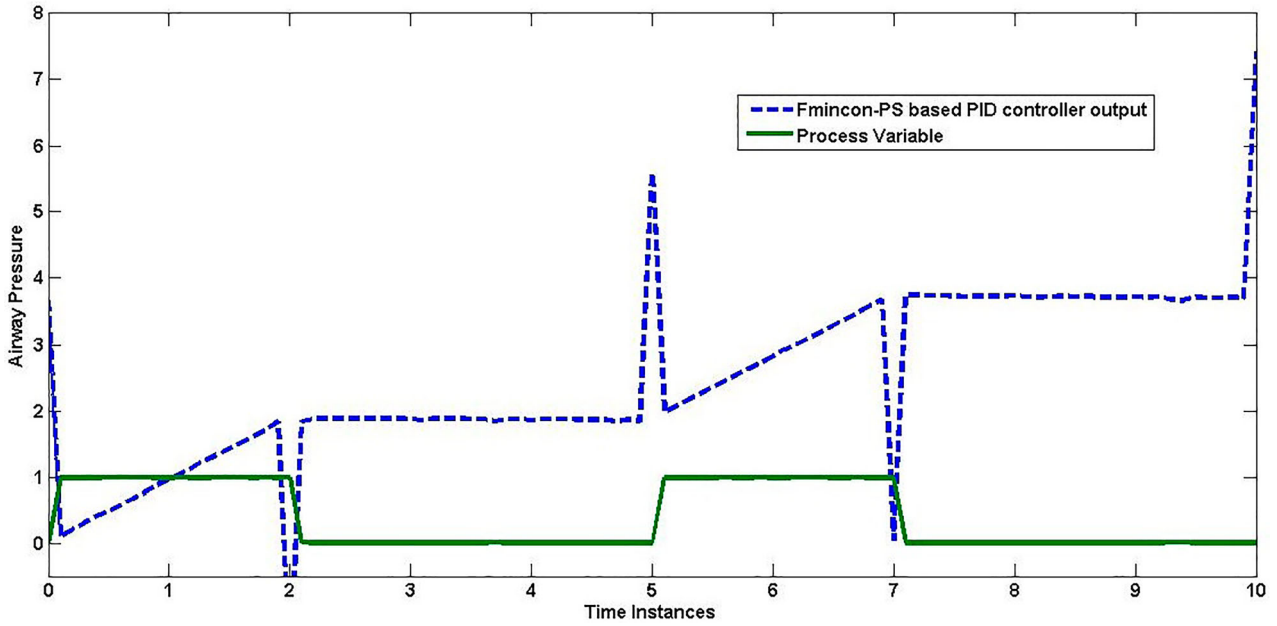


Figure 12. The Controller response vs Process variable of Fmincon-PS based PID controller.

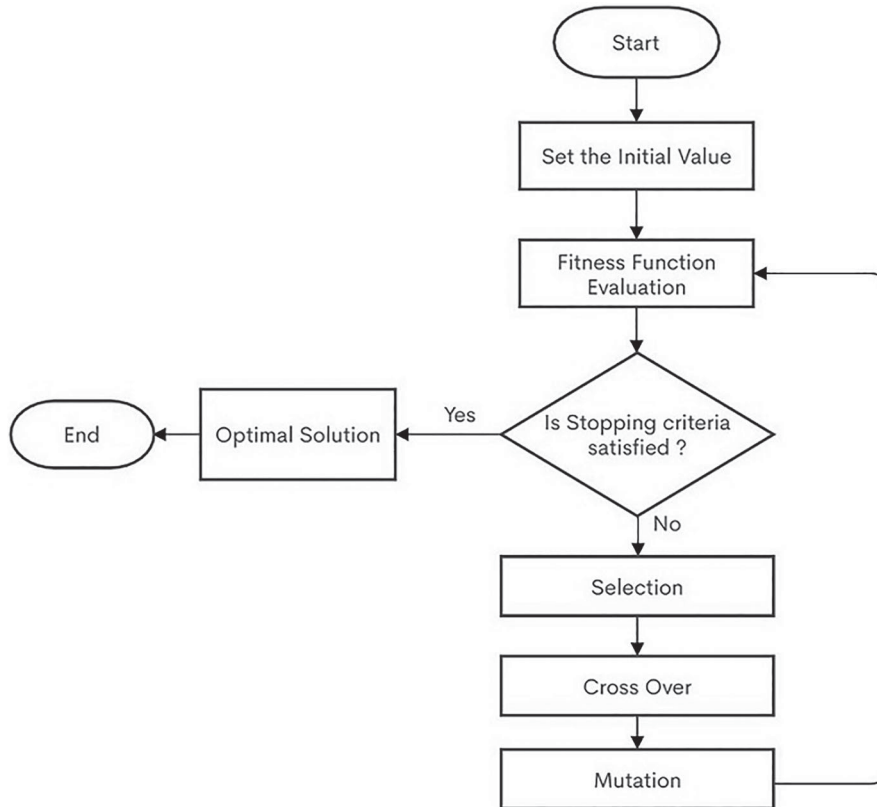


Figure 13. Genetic algorithm flowchart.

based optimization technique [37]. The Flowchart representing the genetic algorithm is shown in Figure 13.

Fractional Order controllers may outperform traditional (integer-order) controllers in terms of system performance and robustness, according to a recent study. The fractional-order PID controller consists of a collection of fractional operators as well as controller gains. As a result, the FOPID controller design approach consists of solving five nonlinear equations with five system unknowns. The complexity of the five

Table 3. Fmincon-PS based PID controller parameters.

Controller	K_p	K_i	K_d
Fmincon-PS based PID	1.225	131.9539	0.025

nonlinear equations, on the other hand, is significant, owing to the fractional order [38].

The FOPID equation is mentioned in Equation (11).

$$G = K_p + \frac{K_i}{S^\lambda} + K_d S^\mu \tag{11}$$

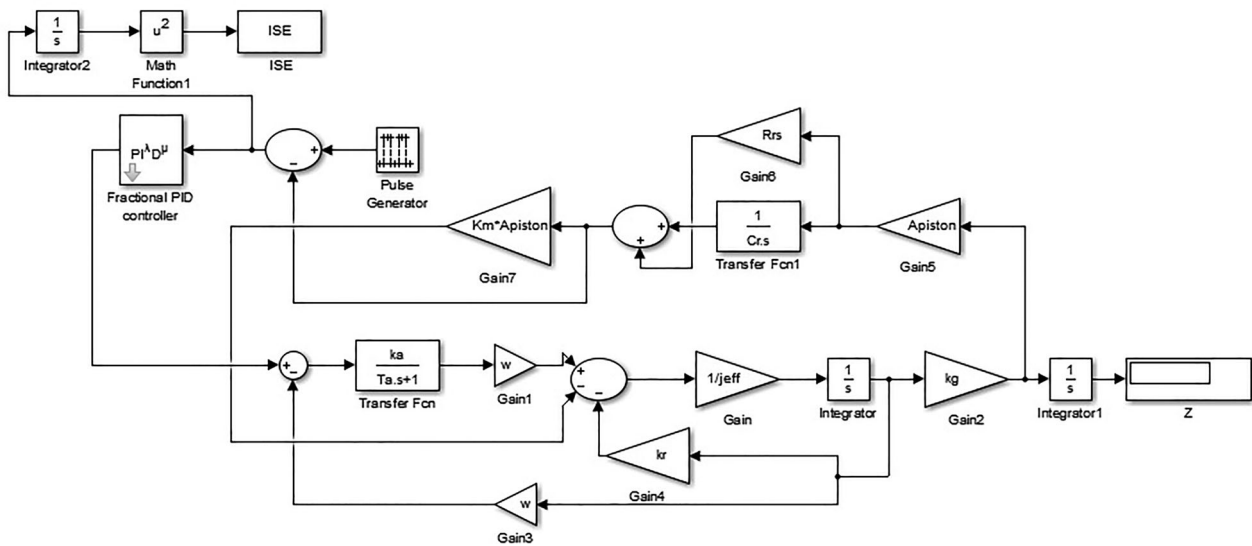


Figure 14. The simulink model of GA based FOPID controller.

The five parameters are tuned by considering the objective function as ISE. The MATLAB Equations (12)–(16) represents the genetic algorithm used for tuning the FOPID parameters.

$$[Kp, fval, exitflag, output] = ga(ISE, nvars, A1, b1, Aeq1, beq1, lb1, ub1) \quad (12)$$

$$[Ki, fval, exitflag, output] = ga(ISE, nvars, A2, b2, Aeq2, beq2, lb2, ub2) \quad (13)$$

$$[\lambda, fval, exitflag, output] = ga(ISE, nvars, A3, b3, Aeq3, beq3, lb3, ub3) \quad (14)$$

$$[Kd, fval, exitflag, output] = ga(ISE, nvars, A4, b4, Aeq4, beq4, lb4, ub4) \quad (15)$$

$$[\mu, fval, exitflag, output] = ga(ISE, nvars, A5, b5, Aeq5, beq5, lb5, ub5) \quad (16)$$

$nvars$ is the number of variables, A , b are the linear inequality constraints matrix and vector, respectively. Aeq and beq are the linear equality constraints matrix and vector, respectively. lb represents the lower bound and ub represents the upper bound for the FOPID parameters. The number of variables used here is 5.

Here, the genetic algorithm-based FOPID controller is implemented where the algorithm is used to find the FOPID parameters. The fitness function is nothing but the objective function that needs to be reduced has to be specified here. The Fitness function's number of independent variables are given in the number of variables [39]. The lower bounds and the upper bounds are the

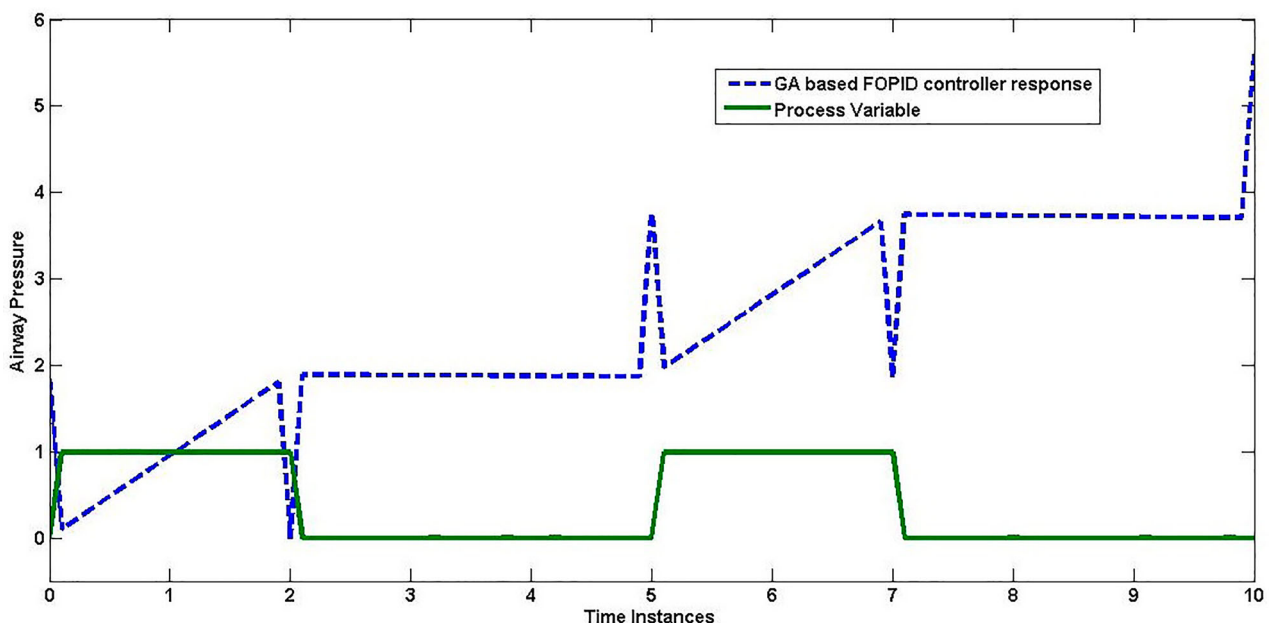


Figure 15. GA based FOPID controller response vs process variable.

lowest and highest values on the variables mentioned in the constraints. Population specifies the choice for the population of the genetic algorithm.

The Population type indicates the choice of the input given for the fitness function. Here, the double vector is chosen that is given for the integer constraints. The Population size indicates how many entities are present in each generation [40]. Here, the population size selected is default 50. The Creation function indicates the function that creates the early population. Here, Constraint dependent is chosen which is uniform when there are 0 linear constraints, or if there are number constraints. The scaling function transforms the fitness function's raw fitness scores into values within the selection function's spectrum of acceptability. Here, the Rank option is selected, which scales the raw scores according to each individual's rank rather than its ranking. An individual's rank is simply their place in the sorted ratings. The power of the distribution of raw scores would be nullified by the Rank fitness scaling. The preference function selects parents for the next generation is based on the fitness scaling function's scaled values. The Tournament is used to choose each parent by randomly chosen people, the number of which is determined by the Tournament size, and then selecting the best child from that group to be a parent. The children are generated by the genetic algorithm at each new generation based on reproduction. The number of individuals who are certain and live to see the next generation is represented by the Elite count. The Elite count is set to be less than or equal to the Population size in positive integers. The Crossover would create a new human child for the next generation by merging two individual parents. While there are no linear constraints, the option dispersed is selected, and when there are linear constraints, the option intermediate is selected. This thing ensures the parent's and children's compatibility [41]. When the population size is set to a vector with a length greater than 1, migration is described as the movement of individuals between the algorithm's subpopulations. The direction of migration will be forwarded into the last sub-population. The nonlinear constraint will be represented by constraint parameters. The starting value for the genetic algorithm is defined by the initial penalty. The first penalty must be equal to or higher than one. The algorithm's termination is determined by the stopping conditions. Generations indicate the number of iterations needed by the genetic algorithm. The time-limit specifies how long the genetic algorithm will run in seconds before the iteration is stopped. If the best fitness value is less than or equal to the Fitness optimum value, the algorithm will terminate. When the average shift in the fitness function value over the Stall generations is less than the Function tolerance, the algorithm will terminate. The algorithm would terminate if the best fitness value does not change within the time interval given by the Stall

Table 4. GA based FOPID controller parameters.

Controller	K_p	K_i	K_d	λ	μ
GA based FOPID	1.8993	130.98	0.00698	0.99	0.503

time limit. When the genetic algorithm is running, the Plot functions will plot different facets of it. On the view window, each one will be plotted on its own axis. The algorithm runs for many numbers of iteration until it gets the best fit values. If there is any issue identified, the algorithm terminates and the reason for termination will be displayed. The best fit value can be used to tune the K_p , K_i , K_d , λ , μ value of the FOPID controller. The MATLAB Simulink model of GA-based FOPID controller is shown in Figure 14. The simulation time is 10 s. PID parameters of GA based FOPID controllers is tabulated in Table 4. The Controller response vs Process variable of GA based FOPID controller is shown in Figure 15.

3.3. Hybrid MPC-PID controller

Combination of Model Predictive Controller-Proportional Integral Derivative controller is a hybrid controller used to control the airway pressure of the artificial respiration system [42]. The Hybrid MPC-PID block diagram is shown in Figure 16.

MPC is a very popular controller that helps to tune the process and removes the issues of the system. It can vary the parameters in the ventilation system simultaneously.

Model prediction at time step k is given in Equation (17).

$$y_k = \sum_{i=1}^{N-1} S_i \Delta u_{k-i} + S_N \Delta u_{k-N} \quad (17)$$

The error generated after comparing the model output and actual output is considered as the input value for the prediction block. The forthcoming value of the output can be expected based on the system input and the error. The optimizer in the calculation block will optimize the predefined objective functions at any sample time to give the upcoming control action based on the set-points, constraints, and prediction values. Control measurements are completed in the time interval called Sampling time (T_s), which is equal to the control interval. The controller calculates the upcoming control action based on the Horizon Prediction (P). To achieve the optimal control action, the objective function must be low.

PID controller is a popular controller used in most of the processes because of its simplicity and wonderful performance [43]. The PID parameters are tuned based on Ziegler Nichols (ZN) method [44,45].

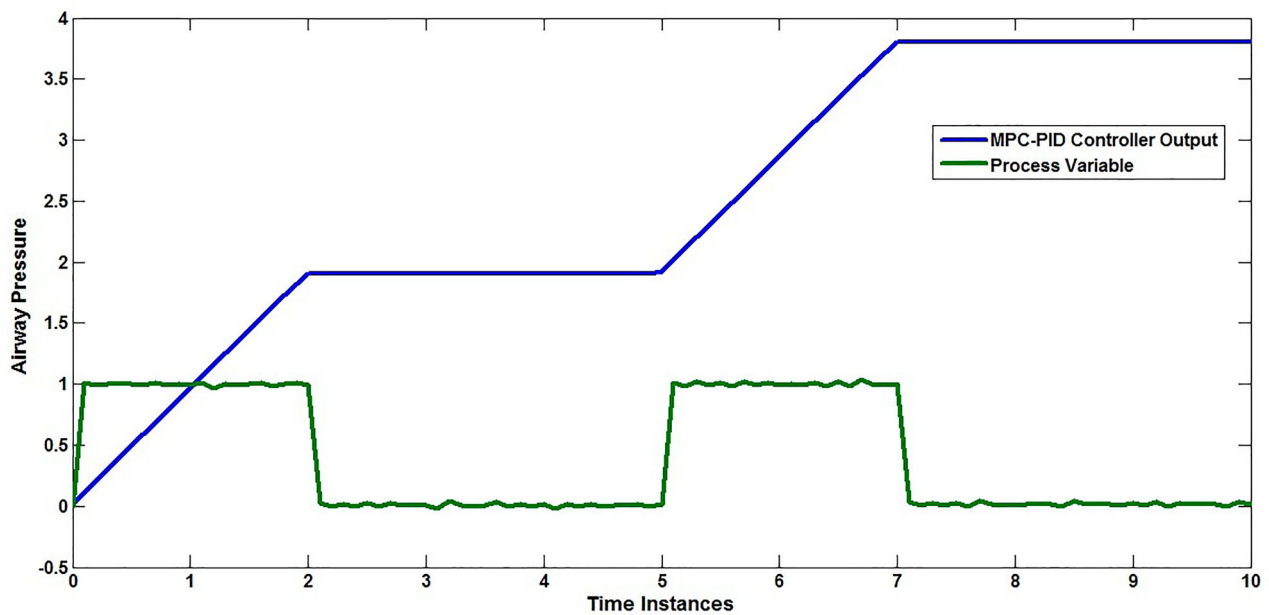


Figure 18. The Controller response vs Process variable of Hybrid MPC-PID controller.

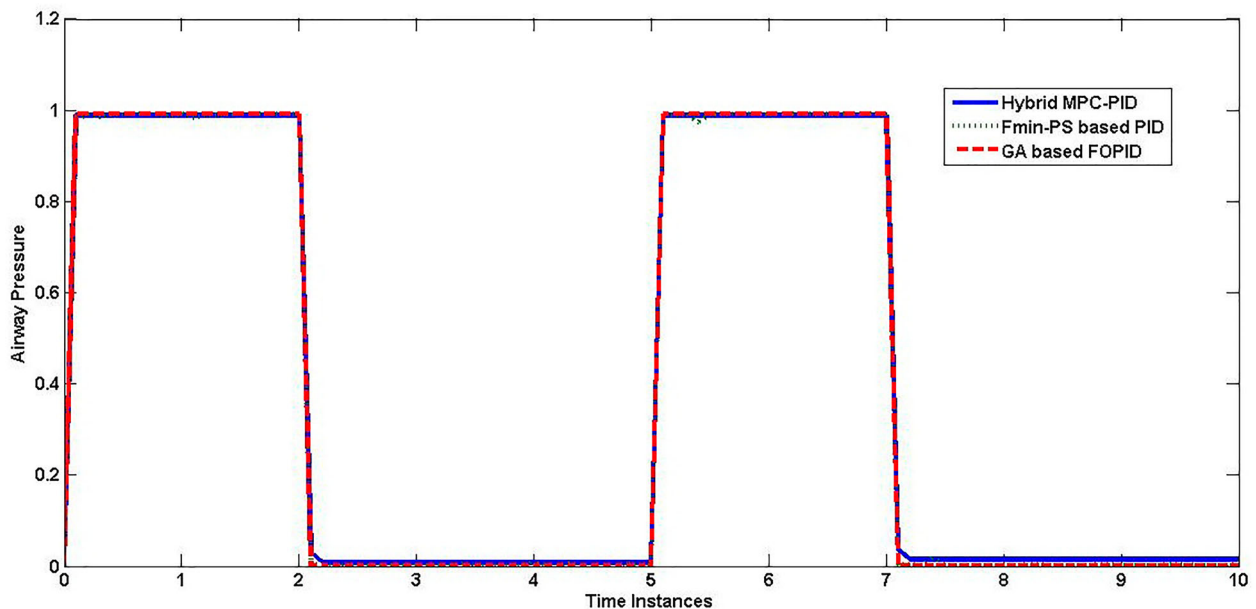


Figure 19. The comparison response of the controller for automatic respiration system.

Table 6. The Time domain specifications the controllers.

Controller	T_r (s)	T_s (s)
Hybrid Fmincon-PS based PID	0.0632	0.95
GA based FOPID	0.0628	0.23
Hybrid MPC-PID	0.0636	0.36

Table 7. The error indices of the controllers.

Controller	ISE	IAE	ITAE
Hybrid Fmincon-PS based PID	0.00518	0.02895	0.1026
GA based FOPID	0.00022	0.029	0.1035
Hybrid MPC-PID	0.04963	0.804	0.1649

for the automatic respiration system. The time-domain specifications: Rise Time (T_r) and Settling Time (T_s) are shown in Table 6. The error indices of the controllers are tabulated in Table 7. From Figure 20, it is found that the controller responds to the input when the patient requires more oxygen at a particular time.

The genetic algorithms search a population of points in parallel. As a result, unlike traditional approaches that search from a single point, it is capable to avoid getting trapped in a local optimal solution. Genetic algorithms employ probabilistic rather than deterministic selection principles. However, the delayed convergence of a genetic algorithm-based FOPID controller

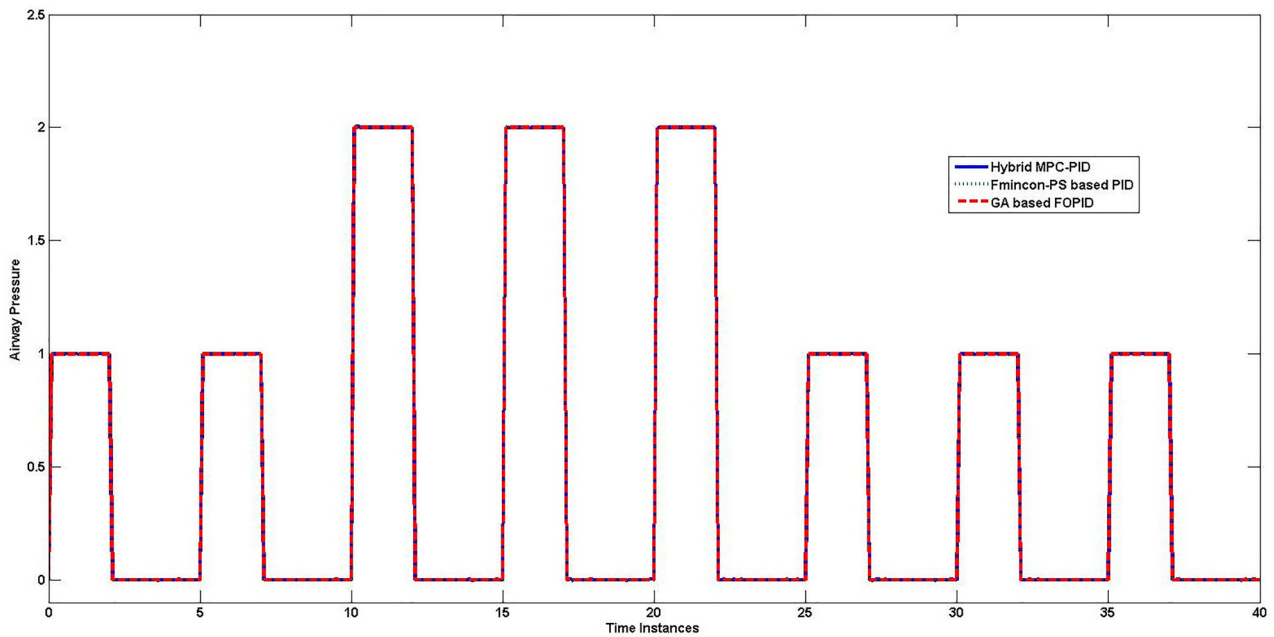


Figure 20. The set-point tracking of the controller for automatic respiration system.

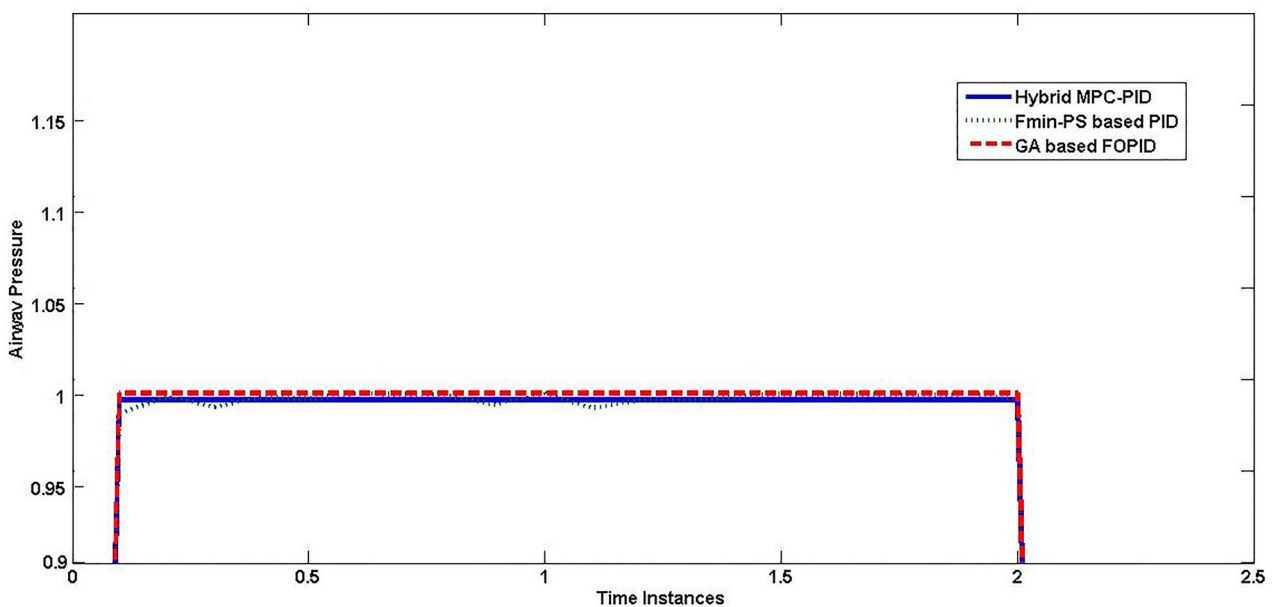


Figure 21. The enlarged controller response for automatic respiration system.

is a major disadvantage. Whereas Fmincon-Pattern-search is a class of numerical optimization methods that do not need the use of a gradient. As a result, it can be applied to non-continuous and non-differentiable functions. But the major drawback of this method is, it is a slow method and is difficult to execute. The settling time of the Fmincon-Pattern search based PID controller is high. MPC-based controllers are more advanced methods used to solve nonlinear problems. But it is more complex and takes time to execute when compared to GA-based FOPID Controllers.

The optimization problem is displayed on a convergence graph to see if it is converging to the best

solution [46]. The convergence diagram of the genetic algorithm and Fmincon-PS algorithm is shown in Figure 22.

From Figure 22, the GA-based FOPID algorithm converged substantially faster than the hybrid Fmincon pattern search algorithm when using the prior airway pressure measurement as an initial population. When compared to the GA-based algorithm with a hybrid Fmincon pattern search algorithm, the GA-based algorithm with historical airway pressure demonstrated a 38% reduction in average delay at iteration 200. This has the potential to significantly enhance airway pressure regulation.

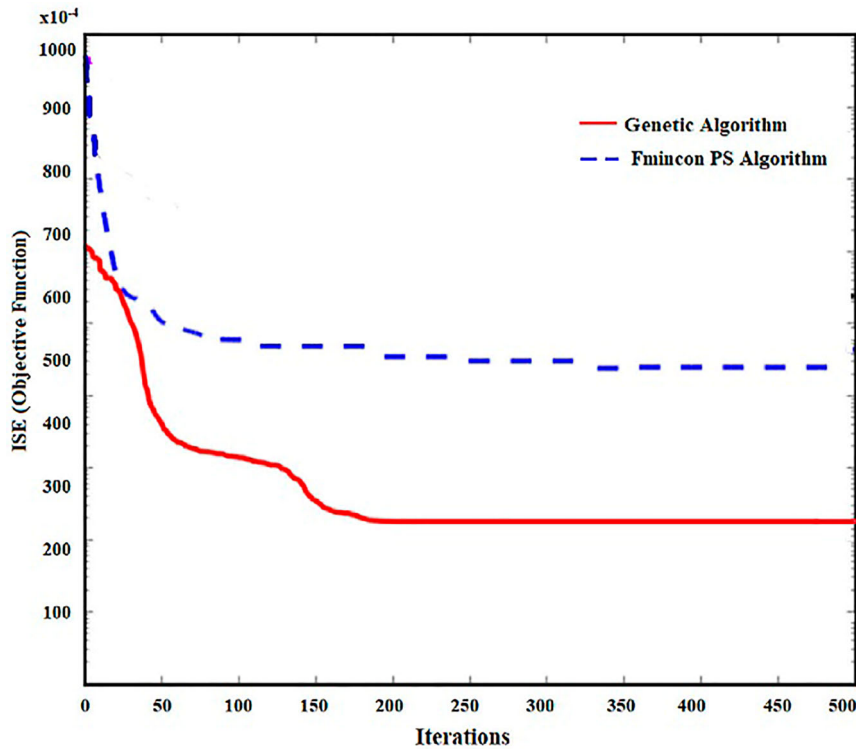


Figure 22. Convergence Comparison: genetic algorithm vs Fmincon-PS algorithm.

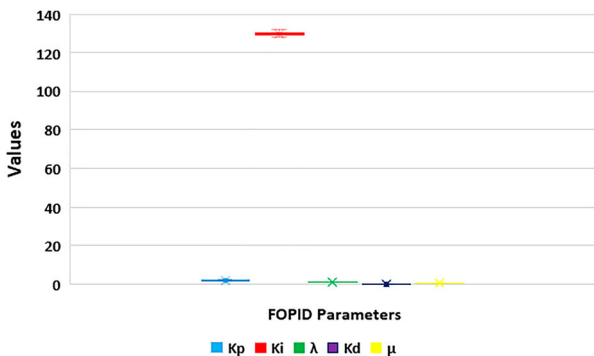


Figure 23. Stability analysis of GA based FOPID controller.

From Table 6, it is observed that the GA-based FOPID controller has efficient set-point tracking which has less rise time and faster settling point when compared to other controllers. From Table 7, it is observed that GA-based FOPID controllers have fewer error values when compared to the other controllers. GA-based FOPID controller gives a fast response with less error, which is very important for the system as the oxygen has to be supplied to the patients immediately when they need it to save their life.

Figure 23 shows the stability analysis of the GA-based FOPID controller plotted in box and whisker plot was taken for 400 iterations. The values of GA-based FOPID parameters lie between the upper and lower bound values. Figure 24 shows the Clear View of Stability of each parameters of GA based FOPID Controller.

5. Conclusion

Based on the result obtained by comparing the hybrid controllers, the genetic algorithm based FOPID controller gives a better response than Hybrid Fmincon-Pattern Search based PID controller and Hybrid MPC-PID controller. From the result and discussion section, it is observed that the integral square error value of the genetic algorithm-based FOPID controller is 0.49% less than Hybrid Fmincon-PS based PID controller and 4.94% lesser than Hybrid MPC-PID controller. The integral absolute error of the genetic algorithm-based FOPID controller is 77.5% less than the Hybrid MPC-PID controller and 0.005% lesser than Hybrid Fmincon-PS based PID controller. The settling time of the genetic algorithm based FOPID controller is 72% faster than Hybrid Fmincon-PS based PID controller and 13% faster than Hybrid MPC-PID controller. The genetic algorithm based FOPID controller improves the set-point tracking capability for various pressure set points. Also, the GA-based FOPID algorithm converged substantially faster than the hybrid Fmincon pattern-search algorithm. The stability analysis of genetic algorithm-based FOPID controller shows that the values are stable and lie within the bounds. So genetic algorithm-based FOPID controller can be used in the Auto Respiration System to supply the required oxygen for the patients within the stipulated time. The limitation of the proposed work is that inadequate patient data may lead to an imperfect model which is difficult to achieve the design criteria. In

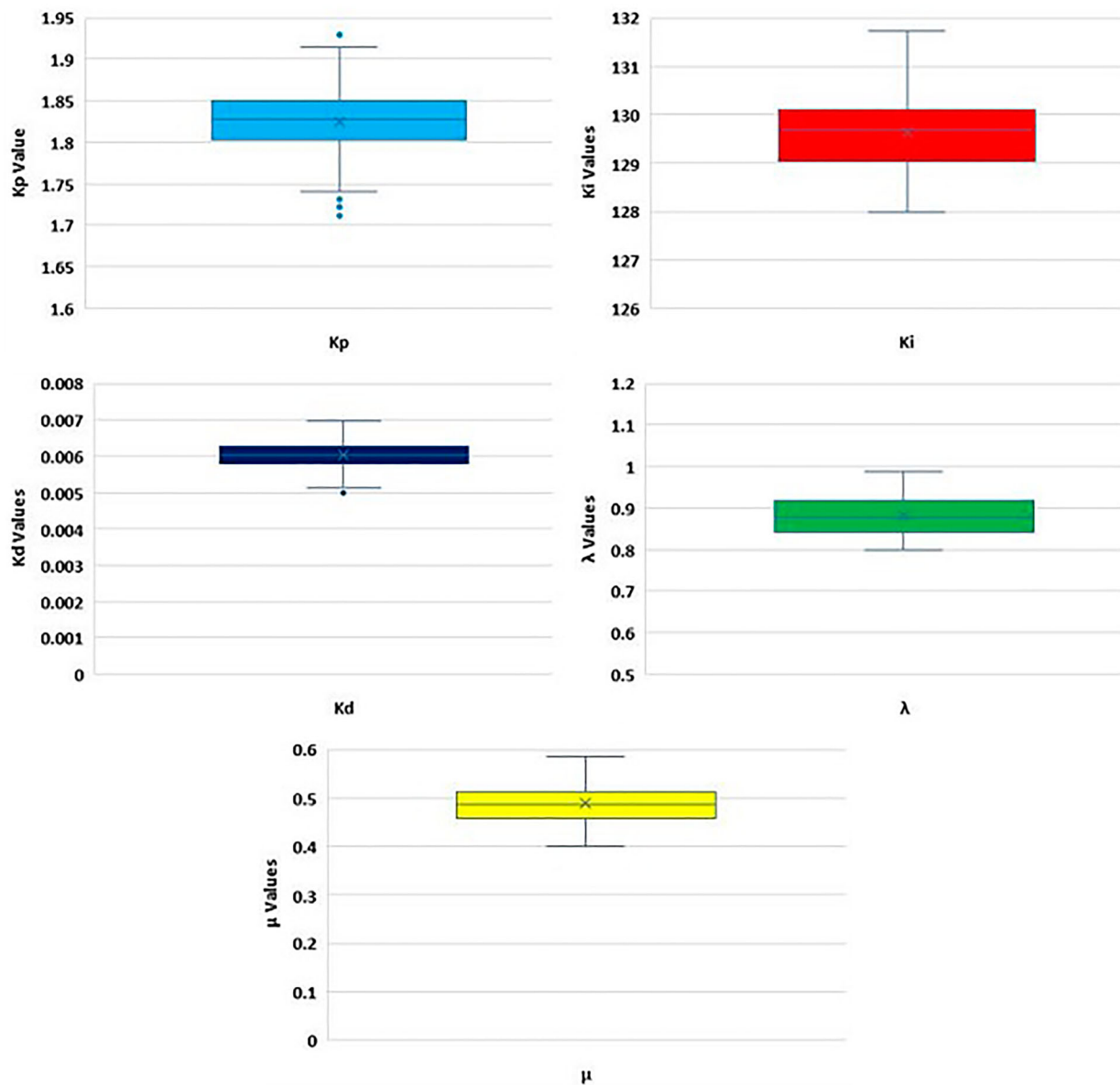


Figure 24. Clear View of Stability of each parameters of GA based FOPID Controller.

the future, a model will be trained using an artificial intelligence-based algorithm for modelling the auto respiration system to get the required pressure value for the corona patients.

Disclosure statement

No potential conflict of interest was reported by the author(s).

Data availability statement

Data sharing is not applicable to this article as no new data were created or analysed in this study.

ORCID

S. Sakthiya Ram  <http://orcid.org/0000-0002-7976-3080>
 C. Kumar  <http://orcid.org/0000-0002-1132-4794>
 A. Ramesh Kumar  <http://orcid.org/0000-0002-8916-3767>
 T. Rajesh  <http://orcid.org/0000-0003-2781-9385>

References

- [1] Singhal T. A review of coronavirus disease-2019 (COVID-19). *Indian J Pediatr.* 2020;87(4):281–286.
- [2] Ye W, Gu W, Guo X, et al. Detection of pulmonary ground-glass opacity based on deep learning computer artificial intelligence. *Biomed Eng Online.* 2019;18(1):1–12.
- [3] Luks AM, Swenson ER. Pulse oximetry for monitoring patients with COVID-19 at home. Potential pitfalls and practical guidance. *Ann Am Thorac Soc.* 2020;17(9):1040–1046.
- [4] Jubran A. Pulse oximetry: review. *Crit Care.* 2015; 19:272.
- [5] Dijemeni ED, Dickinson R. Portable mobile real time oxygen monitoring auto-ventilation system. 21-23 Nov. Iasi, Romania. E-Health and Bioengineering Conference (EHB). 2013.
- [6] Brochard L. Intrinsic (or auto-) PEEP during controlled mechanical ventilation. In: Michael R. Pinsky, Laurent Brochard, Göran Hedenstierna, Massimo Antonelli (eds). *Applied physiology in intensive care medicine 1.* Springer; 2012. p. 3–5.

- [7] Acharya D, Das DK. Swarm optimization approach to design PID controller for artificially ventilated human respiratory system. *Comput Methods Programs Biomed.* 2021;198:105776.
- [8] Xue Y, Xue B, Zhang M. Self-adaptive particle swarm optimization for large-scale feature selection in classification. *ACM Trans Knowl Discov Data (TKDD).* 2019;13(5):1–27.
- [9] Güler H, Türkoğlu İ, Fikret ATA. Mekanik Ventilator Tasarım Metotları. *Erciyes Üniversitesi Fen Bilimleri Enstitüsü Fen Bilimleri Dergisi.* n.d.;26(3):248–257.
- [10] Nemoto T, Hatzakis GE, Thorpe CW, et al. Automatic control of pressure support mechanical ventilation using fuzzy logic. *Am J Respir Crit Care Med.* 1999;160(2):550–556.
- [11] Tehrani F, Rogers M, Lo T, et al. A dual closed-loop control system for mechanical ventilation. *J Clin Monit Comput.* 2004;18(2):111–129.
- [12] Tehrani FT. A closed-loop system for control of the fraction of inspired oxygen and the positive end-expiratory pressure in mechanical ventilation. *Comput Biol Med.* 2012;42(11):1150–1156.
- [13] Zivkovic M, Bacanin N, Venkatachalam K, et al. COVID-19 cases prediction by using hybrid machine learning and beetle antennae search approach. *Sustain Cities Soc.* 2021;66:1–22.
- [14] Bakhsh AA. High-performance in classification of heart disease using advanced supercomputing technique with cluster-based enhanced deep genetic algorithm. *J Supercomput.* 2021;77:10540–10561.
- [15] Jayakar SA, Tamilselvan GM, Sundararajan TVP, et al. Investigation on hybrid optimisation based proportional integral derivative and model predictive controllers for hot air generator. *J Environ Protect Ecol.* 2020;21(4):1414–1425.
- [16] Ferrari A, Mittica A, Pizzo P, et al. PID controller modelling and optimization in CR systems with standard and reduced accumulators. *Int J Autom Technol.* 2018;19(5):771–781.
- [17] Kusnandi J, Stephanus H, Hadi SP. Modelling and simulation for used genetic algorithm method to speed control of three-phase induction motor. *Relation.* 2016;1(22):35–47.
- [18] Bacanin N, Bezdán T, Venkatachalam K, et al. Optimized convolutional neural network by firefly algorithm for magnetic resonance image classification of glioma brain tumor grade. *J Real-Time Image Process.* 2021;18:1085–1098.
- [19] Kim JW, Heise RL, Reynolds AM, et al. Aging effects on airflow dynamics and lung function in human bronchioles. *PLoS ONE.* 2017;12(8):1–20.
- [20] Ogunnaike BA, Willis Harmon Ray. *Process Dynamics, Modeling, and Control.* Oxford University Press; 1994.
- [21] Shi Y, Wang Y, Cai M, et al. An aviation oxygen supply system based on a mechanical ventilation model. *Chin J Aeronaut.* 2018;31(1):197–204.
- [22] Pan I, Das S, Gupta A. Tuning of an optimal fuzzy PID controller with stochastic algorithms for networked control systems with random time delay. *ISA Trans.* 2011;50(1):28–36.
- [23] Gaing ZL. A particle swarm optimization approach for optimum design of PID controller in AVR system. *IEEE Trans Energy Convers.* 2004;19(2):384–391.
- [24] Walter M, Leonhardt S. Control applications in artificial ventilation. In: 2007 Mediterranean Conference on Control & Automation, Athens, Greece. 2007; IEEE. p. 1–6.
- [25] Sunil PU, Barve J, Nataraj PSV. Mathematical modeling, simulation and validation of a boiler drum: some investigations. *Energy.* 2017;126:312–325.
- [26] Åström KJ, Bell RD. Simple drum-boiler models. In: *Power systems: modelling and control applications.* Elsevier; 1989. p. 123–127.
- [27] Kumar D, Meenakshipriya B, Ram SS. Design and comparison of intelligent controllers for a boiler drum level system. *Int J Appl Eng Res.* 2015;10(93):299–303.
- [28] Albaghdadi AM, Baharom MB, Sulaiman SAB. Parameter design optimization of the crank-rocker engine using the FMINCON function in MATLAB. In: *IOP Conference Series: Materials Science and Engineering, Vol. 1088.* IOP Publishing; 2021. p. 1–8.
- [29] Valluru SK, Kumar R, Kumar R. Design and real time implementation of fmincon, MOGA tuned IO-PID and FO-PI λ D μ controllers for stabilization of TRMS. *Procedia Comput Sci.* 2020;171:1241–1250.
- [30] Baek SS, Choi DH, Jung JW, et al. Optimizing low impact development (LID) for stormwater runoff treatment in urban area, Korea: experimental and modeling approach. *Water Res.* 2015;86:122–131.
- [31] Soni V, Parmar G, Kumar M. A hybrid grey wolf optimisation and pattern search algorithm for automatic generation control of multi-area interconnected power systems. *Int J Adv Intell Paradig.* 2021;18(3):265–293.
- [32] Wahid F, Ghazali R. Hybrid of firefly algorithm and pattern search for solving optimization problems. *Evol Intell.* 2019;12(1):1–10.
- [33] Sahu RK, Panda S, Padhan S. A hybrid firefly algorithm and pattern search technique for automatic generation control of multi area power systems. *Int J Electr Power Energy Syst.* 2015;64:9–23.
- [34] Kaliappan V. Nonlinear PID controller parameter optimization using enhanced genetic algorithm for nonlinear control system. *J Control Eng Appl Inf.* 2016;18(2):3–10.
- [35] Pereira FH, Alves WAL, Koleff L, et al. A two-level genetic algorithm for large optimization problems. *IEEE Trans Magn.* 2014;50(2):733–736.
- [36] Shehu GS, Çetinkaya N. A comparison of improved nature-inspired algorithms for optimal power dispatch. *J Control Eng Appl Inf.* 2018;20(4):50–59.
- [37] Norsahperi NMH, Danapalasingam KA. Particle swarm-based and neuro-based FOPID controllers for a Twin Rotor System with improved tracking performance and energy reduction. *ISA Trans.* 2020;102:230–244.
- [38] Al-Dhaifallah M, Kanagaraj N, Nisar KS. Fuzzy fractional-order PID controller for fractional model of pneumatic pressure system. *Math Probl Eng.* 2018;2018:1–9.
- [39] Jayabal S, Natarajan U. Optimization of thrust force, torque, and tool wear in drilling of coir fiber-reinforced composites using Nelder–Mead and genetic algorithm methods. *Int J Adv Manuf Technol.* 2010;51(1–4):371–381.
- [40] Marfoli A, Nardo MD, Degano M, et al. Rotor design optimization of squirrel cage induction motor-Part I: problem statement. *IEEE Trans Energy Convers.* 2020;36:1271–1279.

- [41] Jahanshahi H, Sari NN. On the computational analysis of the genetic algorithm for attitude control of a carrier system. In: Intelligent System. IntechOpen; 2018.
- [42] Singh R, Sen M, Ierapetritou M, et al. Integrated moving horizon-based dynamic real-time optimization and hybrid MPC-PID control of a direct compaction continuous tablet manufacturing process. *J Pharm Innov.* 2015;10(3):233–253.
- [43] Khodadadi H, Ghadiri H. Fuzzy logic self-tuning PID controller design for ball mill grinding circuits using an improved disturbance observer. *Min Metall Explor.* 2019;36(6):1075–1090.
- [44] Nascu I. Development and evaluation of a PID auto-tuning algorithm based on relay feedback. *J Control Eng Appl Inf.* 2002;4(3):39–46.
- [45] Jain S, Hote YV. Design of FOPID controller using BBBC via ZN tuning approach: simulation and experimental validation. *IETE J Res.* 2020;66:1–15.
- [46] Xi C, Mai VS, Xin R, et al. Linear convergence in optimization over directed graphs with row-stochastic matrices. *IEEE Trans Autom Control.* 2018;63(10):3558–3565.